JBIC Journal of Biological Inorganic Chemistry (2024) 29:315–330
https://doi.org/10.1007/s00775-024-02059-9

ORIGINAL PAPER

Synthesis, in vitro antitumor evaluation and structure activity relationship of heptacoordinated amino-*bis*(Phenolato) Ti(IV) complexes stabilized by 2,6-dipicolinic acid

Shanjia Li[1] · Xupeng Zhang[1] · Tiankun Zhao[1] · Nan Liu[1] · Yong Zhang[1] · Peng Wang[2] · Zhongduo Yang[1] · Thomas Huhn[3]

Received: 10 November 2023 / Accepted: 22 February 2024 / Published online: 9 May 2024

Abstract

Eighteen novel Ti(IV) complexes stabilized by different chelating amino-*bis*(phenolato) (ONNO, ONON, ONOO) ligands and 2,6-dipicolinic acid as a second chelator were synthesized with isolated yields ranging from 79 to 93%. Complexes were characterized by ^{1}H and ^{13}C-NMR spectroscopy, as well as by HRMS and X-Ray diffraction analysis. The good to excellent aqueous stability of these Ti(IV) complexes can be modulated by the substitutions on the 2-position of the phenolato ligands. Most of the synthesized Ti(IV) complexes demonstrated potent inhibitory activity against Hela S3 and Hep G2 tumor cells. Among them, the naphthalenyl based Salan type **2j**, 2-picolylamine based [ONON] type **2n** and *N*-(2-hydroxyethyl) based [ONOO] type **2p** demonstrated up to 40 folds enhanced cytotoxicity compared to cisplatin together with a significantly reduced activity against healthy AML12 cells. The three Ti(IV) complexes exhibited fast cellular uptake by Hela S3 cells and induced almost exclusively apoptosis. **2j** could trigger higher level of ROS generation than **2p** and **2n**.

Graphical abstract

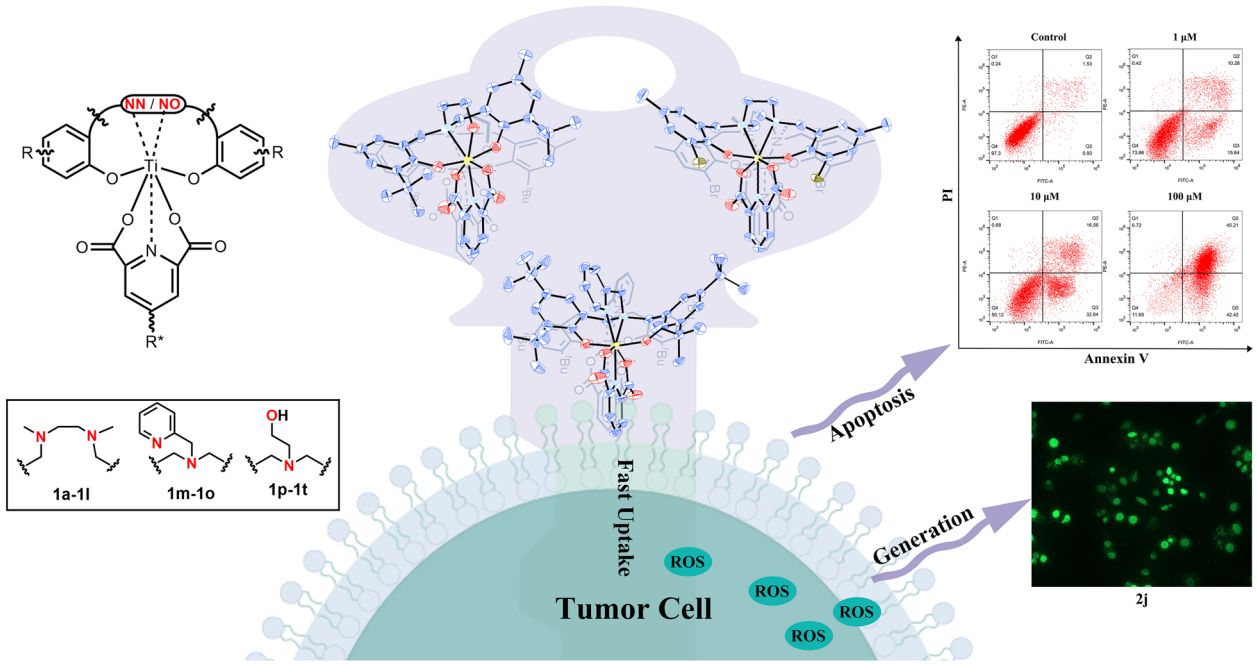

Shanjia Li and Xupeng Zhang have contributed equally to this work.

Extended author information available on the last page of the article

Keywords Titanium complexes · Amino-*bis*(Phenolato) ligands · Anti-tumor · Aqueous stability · 2,6-Dipicolinic acid

Introduction

Metal based coordination complexes exhibit unique advantages compared to organic compounds in drug R&D such as flexible conformation, nuclide imaging and the ability to react with biological targets via ligand exchange [1]. Of metallic complexes with anti-tumor activity, platinum (Pt) based complexes have achieved remarkable success in the treatment of malignant tumors ever since the milestone-drug cisplatin was approved by FDA in the 1970s [2–4]. However, platinum drugs are associated with systemic side effects and drug resistance generated from long-time clinical use [5]. Hence, a vast number of non-platinum metallic complexes have been synthesized and evaluated for antitumor efficacy [6–8], among which the titanium (Ti, group IVB) complexes have attracted much attention because two Ti(IV) complexes, titanocene dichloride (**[$Cp_2Ti(IV)Cl_2$]**, TDC) [9] and budotitane (*cis*-diethoxybis(1-phenylbutane-1,3-dionato)Ti(IV)) [10] entered clinical trials in the 1980s [11]. However these two Ti(IV) complexes and their derivatives suffered from insufficient aqueous stability and undefined mechanism of action [12]. In 2007, Tshuva *et.al.* reported the anti-tumor evaluation of diamino-*bis*(phenolato) (Salan) stabilized Ti(IV) *bis*-alkoxyl complexes, which were found to exhibit enhanced aqueous stability and transferrin independent cell membrane penetrating ability [13, 14]. Their antitumor spectrum, structure–activity relationship and anti-tumor active species were reported in later studies [15].

Changing the 'classical' dianionic tetradentate Salan to a tetraanionic hexadentate Salan gave new homoleptic phenolato Ti(IV) complexes with exceedingly good aqueous stability [16]. These Salan ligands feature two additional (*N*-(2-hydroxyethyl)) donors in their backbone, thus tightly coordinating Ti(IV). The most prominent Ti(IV) complex, 'PhenolaTi' named by the group of Tshuva *et.al.*, showed significantly enhanced inhibitory effect against a number of tumor cells compared to cisplatin and very little side effects on mouse' spleen and kidney cells [17]. A synergistic effect was found when they were used in combination with cisplatin [18]. After nano-formulation, they were stable in gastric acid and had comparable treatment effects in CDX model mice when administered orally rather than injected [19]. An even higher coordinated class of titanium complexes was already presented in 2012 by Huhn et al. [20]. These complexes are based on the concept of *bis*-chelation and utilize 2,6-dipicolinic acid (Dipic), a dianionic tridentate, as a second chelator in addition to a conventional Salan ligand. The resulting heptacoordinated heteroleptic Ti(IV) Salan-complexes showed exceedingly good aqueous stability and excellent antitumor activity both in vitro and in vivo [20, 21]. A radioiostopic **[Ti^{45}][SalanTi(IV)Dipic]** with diagnosing features was successfully synthesized inspired by this ligand system [22]. Recently we reported a facile protocol for efficient synthesis of Salan Ti(IV) *bis*-chelates in green solvents in just 90 s [23], and also an efficient functionalization route for these Ti(IV) *bis*-chelates via Sonogashira reaction [24]. However, the compound library of Salan Ti(IV) *bis*-chelates consists only of ten molecules bearing limited substitution patterns [25]. Hence, we became interested to enhance the molecular diversity through employing different phenolato ligands as well as by modifications of the ethylenediamine backbone (Scheme 1). Our aim is to improve the understanding of structure–activity relationships and to identify new Ti(IV) complexes with potent anti-tumor activity.

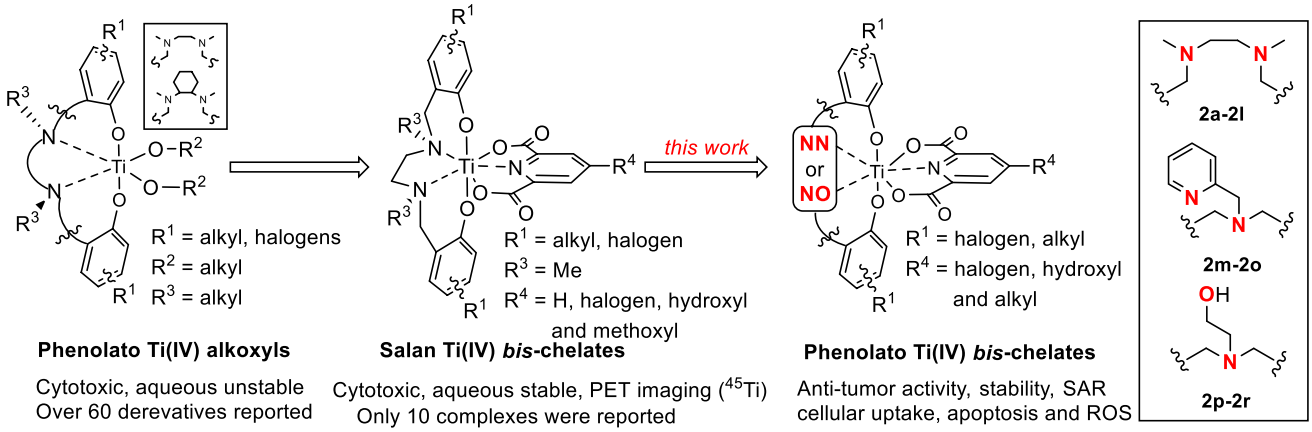

Scheme 1. Diamino-*bis*(phenolato) Ti(IV) complexes with anti-tumor activity

In fact, two types of phenolato Ti(IV) *bis*-chelates have been reported. These are either of the [ONNO] (Salan) or [ONON]-type [25]. It has been shown that anti-tumor activity of these is primarily influenced by substitutions at the phenolato ligands [21, 23]. Steric demanding *t*-butyl groups on the phenolato 2-position resulted in vanished antitumor activity. This was thought to be due to excessive shielding of the Ti(IV) center, as the Ti(IV) complexes remained stable in buffered solutions at pH as low as 1.9 and up to 12.1 [21]; Ti(IV) *bis*-chelates bearing $Salan^{2,4-Cl}$ demonstrated significantly enhanced antitumor activity than $Salan^{4-I}$ and $Salan^{2,4-Me}$ [21, 24]; Electron deficient groups (CF_3 or sulfonamide) on the Salan lead to decreased aqueous stability but enhanced anti-tumor activity [21, 26]; A thiol-bridged Salan Ti(IV) *bis*-chelate decomposed fast in H_2O and was completely inactive [21]; Functionalization on the Dipic (4-methoxyl or 4-hydroxyethyl) showed insignificant influence to the anti-tumor activity [21]. No other structural similar phenolato ligands have been explored so far and little is known on the structure activity relationship and mechanism of action of the reported Salan type Ti(IV) *bis*-chelates. Herein, we report the synthesis and anti-tumor evaluation of novel heteroleptic Ti(IV) *bis*-chelates with differently substituted [ONNO] (Salan), [ONON] and [ONOO] type backbone and Dipic as a secondary chelator. In case of the [ONON] and [ONOO] type *bis*-phenolates, the typical ethylenediamine linker of the Salan was replaced by either 2-picolylamino or 2-hydroxyethylamino bridges. Comparison of the aqueous stability of resulting Ti(IV) complexes, induction of apoptosis, cellular uptake and ROS (Reactive oxygen species) generation are also presented.

Experimental section

Representative synthetic procedures

Synthetic procedure for **1a** [27] (6,6'-((ethane-1,2-diylbis(methylazanediyl))*bis*(methylene))*bis*(2,4-difluorophenol)): 2,4-Difluorophenol (1.30 g, 10 mmol) was dissolved in methanol (15 mL), formaldehyde (2 mL, 36% in water) and N, N'-dimethylethylenediamine (0.44 g, 5 mmol) were added at once. The mixture was then heated to reflux for 5 h. Upon completion, the reaction was allowed to cool to r.t., the precipitated **1a** was collected by filtration as a white solid (894 mg, 2.4 mmol, 48%). M.p.: 176 °C. ^{1}H-NMR (600 MHz, $CDCl_3$) δ 6.76 (ddd, J = 11.2, 8.5, 2.6 Hz, 2H, H_{ar}), 6.50 (d, J = 8.5 Hz, 2H, H_{ar}), 3.70 (s, 4H, NCH_2C_{ar}), 2.69 (s, 4H, NCH_2CH_2N), 2.32 (s, 6H, NCH_3); ^{13}C-NMR (151 MHz, $CDCl_3$) δ 154.7 (dd, J = 239.5, 11.0 Hz, C_{ar}), 150.7 (dd, J = 246.8, 12.1 Hz, C_{ar}), 142.0 (dd, J = 12.4, 3.3 Hz, C_{ar}), 123.8 (dd, J = 8.3, 4.0 Hz, C_{ar}), 109.9 (dd, J = 23.0, 3.5 Hz, C_{ar}), 103.9 (dd, J = 26.4, 22.2 Hz, C_{ar}), 61.2 (NCH_2C_{ar}), 54.1 (NCH_2CH_2N), 41.8 (NCH_3); ^{19}F-NMR (400 MHz, $CDCl_3$) δ -133.9 (FC_{ar}), -123.2 (FC_{ar}). HRMS (ESI-TOF) m/z Calcd for $C_{18}H_{21}F_4N_2O_2$ $[M+H]^+$: 373.1534. Found: 373.1536. Anal. Calcd for $C_{18}H_{20}F_4N_2O_2$: 58.06% (C); 5.41% (H), Found: 58.31% (C); 5.26% (H).

Synthetic procedure for **1j** [28] (1,1'-((ethane-1,2-diylbis(methylazanediyl))*bis*(methylene))*bis*(naphthalen-2-ol)): 2-Naphthol (1.44 g, 10 mmol) was dissolved in methanol (15 mL), formaldehyde (2 mL, 36% in water) and N, N'-dimethylethylenediamine (0.44 g, 5 mmol) were added at once. The mixture was then heated to reflux for 5 h. Upon completion, the reaction was allowed to cool to r.t., the precipitated **1j** was collected by filtration as a white solid (1.84 g, 4.6 mmol, 92%). M.p.: 162 °C.^{1}H-NMR (400 MHz, DMSO-d_6) δ 9.11 (s, 2H, OH), 7.89 (d, J = 8.7 Hz, 2H, H_{ar}), 7.71 (d, J = 7.8 Hz, 2H, H_{ar}), 7.65 (d, J = 8.7 Hz, 2H, H_{ar}), 7.32 (dd, J = 6.8, 8.6 Hz, 2H, H_{ar}), 7.19 (dd, J = 6.8, 7.8 Hz, 2H, H_{ar}), 7.02 (d, J = 8.7 Hz, 2H, H_{ar}), 3.99 (s, 4H, NCH_2C_{ar}), 2.68 (s, 4H, NCH_2CH_2N), 2.15 (s, 6H, NCH_3); ^{13}C-NMR (101 MHz, DMSO-d_6) δ 155.8 (C_{ar}), 133.6 (C_{ar}), 129.3 (C_{ar}), 128.8 (C_{ar}), 128.5 (C_{ar}), 126.6 (C_{ar}), 123.0 (C_{ar}), 122.8 (C_{ar}), 118.9 (C_{ar}), 113.7 (C_{ar}), 54.5 (NCH_2C_{ar}), 54.2 (NCH_2CH_2N), 41.7 (NCH_3). HRMS (ESI-TOF) m/z Calcd for $C_{26}H_{29}N_2O_2$ $[M+H]^+$: 401.2224. Found: 401.2226. Anal. Calcd for $C_{26}H_{28}N_2O_2$: 77.97% (C); 7.05% (H), Found: 77.69% (C); 6.87% (H).

Synthetic procedure for **1n** [29] (6,6'-(((pyridin-2-ylmethyl)azanediyl)*bis*(methylene))*bis*(2,4-di-*tert*-butylphenol)): **1n** was prepared following the same procedure as for **1j** by using 2,4-di-*tert*-butylphenol (2.06 g, 10 mmol), formaldehyde (2 mL, 36% in water) and 2-picolylamine (0.54 g, 5 mmol) for 24 h as a white solid (2.32 g, 4.3 mmol, 85%). M.p.: 175 °C. ^{1}H-NMR (400 MHz, $CDCl_3$) δ 10.56 (s, 2H, OH), 8.70 (d, J = 4.5 Hz, 1H, H_{pyr}), 7.70 (dd, J = 7.6, 1.0 Hz, 1H, H_{pyr}), 7.29 (t, J = 6.0 Hz, 1H, H_{pyr}), 7.24 (d, J = 2.3 Hz, 2H, H_{ar}), 7.14 (d, J = 7.6 Hz, 1H, H_{pyr}), 6.94 (d, J = 2.3 Hz, 2H, H_{ar}), 3.86 (s, 6H, NCH_2), 1.41 (s, 18H, $(CH_3)_3$), 1.30 (s, 18H, $(CH_3)_3$); ^{13}C-NMR (101 MHz, $CDCl_3$) δ 154.0 (C_{ar}), 148.3 (C_{ar}), 140.6 (C_{ar}), 137.4 (C_{ar}), 136.5 (C_{ar}), 125.3 (C_{ar}), 123.6 (C_{ar}), 122.6 (C_{ar}), 121.4 (C_{ar}), 56.9 (NCH_2), 55.5 (NCH_2), 35.2 ($C_{ar}CH_2$), 34.3 ($C_{ar}CH_2$), 31.8 ($CH_3)_3$), 29.8 ($CH_3)_3$). HRMS (ESI-TOF) m/z Calcd for $C_{36}H_{53}N_2O_2$ $[M+H]^+$: 545.4102. Found: 545.4106. Anal. Calcd for $C_{36}H_{52}N_2O_2$: 79.36% (C); 9.62% (H), Found: 79.65% (C); 9.85% (H).

Synthetic procedure for **1p** [30] (6,6′-(((2-hydroxyethyl)azanediyl)*bis*(methylene))*bis*(2,4-dimethylphenol)): **1p** was prepared following the same procedure as for **1j** by using 2,4-dimethylphenol (1.22 g, 10 mmol), formaldehyde (2 mL, 36% in water) and 2-ethanolamine (0.31 g, 5 mmol) for 24 h as a faint yellow oil (1.33 g, 4.6 mmol, 81%). ^{1}H-NMR (400 MHz, $CDCl_3$) δ 6.71 (s, 2H, H_{ar}), 6.55 (s, 2H,

H_{ar}), 3.75 (t, J = 5.1 Hz, 2H, OCH_2C), 3.61 (s, 4H, $C_{ar}CH_2$), 2.58 (t, J = 5.1 Hz, 2H, OCH_2C), 2.11 (s, 6H, CH_3), 2.08 (s, 6H, $C_{ar}CH_3$); ^{13}C-NMR (101 MHz, $CDCl_3$) δ 152.2 (C_{ar}), 131.4 (C_{ar}), 128.7 (C_{ar}), 128.4 (C_{ar}), 125.1 (C_{ar}), 121.7 (C_{ar}), 60.9 (CH_2OH), 55.8 ($N\underline{C}H_2C_{ar}$), 51.5 (NCH_2), 20.6 (CH_3), 16.2 (CH_3). HRMS (ESI-TOF) m/z Calcd for $C_{20}H_{28}NO_3$ $[M+H]^+$: 330.2064. Found: 330.2068. Anal. Calcd for $C_{20}H_{27}NO_3$: 72.92% (C); 8.26% (H), Found: 72.76% (C); 8.38% (H).

Synthetic procedure for **2a**: To a solution of **1a** (300 mg, 0.84 mmol) in 10 mL THF, Ti(O^iPr)$_4$ (0.25 mL, 0.84 mmol) was added and the reaction was stirred at r.t. for 15 min. Dipic (153 mg, 0.92 mmol) was then added directly to the mixture and the reaction was continued stirring at r.t. for 6 h while monitoring the reaction-progress by TLC. Upon completion, THF was removed by distillation in *vacuo* at 40 °C, the crude compound was purified by chromatography (eluent: $MeOH/CH_2Cl_2$ = 1:40) on silica gel to obtain the pure product as a red solid (455 mg, 0.78 mmol, 93%). M.p.: 301 °C; IR absorptions (cm^{-1}, ATR): 1841, 1634, 1534, 1403, 1306, 1206, 1141, 1086, 1020, 913, 697, 637; ^{1}H-NMR (600 MHz, $CDCl_3$) δ 8.32–8.30 (m, 1H, H_{Pyr}), 8.21 (d, J = 7.8 Hz, 2H, H_{Pyr}), 6.67–6.64 (m, 2H, H_{ar}), 6.57 (d, J = 6.6 Hz, 2H, H_{ar}), 5.39 (d, J = 14.4 Hz, 2H, NCH_2C_{ar}), 3.36 (d, J = 9.0 Hz, 2H, NCH_2CH_2N), 3.25 (d, J = 15.0 Hz, 2H, NCH_2C_{ar}), 2.81 (s, 6H, NCH_3), 2.30 (d, J = 9.0 Hz, 2H, NCH_2CH_2N); ^{13}C-NMR (151 MHz, $CDCl_3$) δ 168.8 (C=O), 155.9 (dd, J = 10.6, 243.1 Hz, C_{ar}), 149.4 (C_{ar}), 149.2 (dd, J = 12.5, 251.7 Hz, C_{ar}), 144.0 (dd, J = 3.5, 12.8 Hz, C_{ar}), 143.9 (C_{ar}), 130.0 (d, J = 10.0 Hz, C_{ar}), 126.1 (C_{ar}), 111.1 (dd, J = 5.7, 23.1 Hz, C_{ar}), 103.9 (dd, J = 22.5, 26.6 Hz, C_{ar}), 63.5 (NCH_2C_{ar}), 53.9 (NCH_2CH_2N), 47.2 (NCH_3); ^{19}F-NMR (400 MHz, $CDCl_3$) δ -131.9 (FC_{ar}), -123.0 (FC_{ar}); UV–*vis* (THF): λ_{max} (ε) = 385 nm; HRMS (ESI-TOF) m/z Calcd for $C_{25}H_{22}F_4N_3O_6Ti$ $[M+H]^+$: 584.0919. Found: 584.0921. Anal. Calcd for $C_{25}H_{21}F_4N_3O_6Ti$: 51.48% (C); 3.63% (H), Found: 51.43% (C); 3.62% (H). Complexes **2b**-**2r** were synthesized following the same procedures as for **2a**.

Synthetic procedure for **2j**: Following the same procedure as for **2a** with **1j** (300 mg, 0.75 mmol) and Ti(O^iPr)$_4$ (0.22 mL, 0.75 mmol) in 10 mL THF for 15 min. Dipic (139 mg, 0.83 mmol) for 3 h to give **2j** as a red solid (425 mg, 0.69 mmol, 93%). M.p.: 242 °C; IR absorptions (cm^{-1}, ATR): 1711, 1604, 1543, 1493, 1415, 1132, 1103, 1040, 880, 846, 634; ^{1}H-NMR (600 MHz, $CDCl_3$) δ 8.29–8.26 (m, 1H, H_{Pyr}), 8.22 (d, J = 6.6 Hz, 2H, H_{Pyr}), 7.84 (d, J = 7.2 Hz, 2H, H_{ar}), 7.74 (d, J = 7.8 Hz, 2H, H_{ar}), 7.59 (d, J = 9.0 Hz, 2H, H_{ar}), 7.47 (t, J = 8.4 Hz, 2H, H_{ar}), 7.33 (t, J = 7.8 Hz, 2H, H_{ar}), 6.74 (d, J = 9.0 Hz, 2H, H_{ar}), 5.39 (d, J = 15.0 Hz, 2H, NCH_2C_{ar}), 4.13 (d, J = 15.0 Hz, 2H, NCH_2C_{ar}), 3.44 (d, J = 9.6 Hz, 2H, NCH_2CH_2N), 2.98 (s, 6H, NCH_3), 2.18 (d, J = 9.0 Hz, 2H, NCH_2CH_2N); ^{13}C-NMR (151 MHz, $CDCl_3$) δ 169.1 (C=O), 157.4 (C_{ar}), 149.8 (C_{ar}), 143.4 (C_{ar}), 132.7 (C_{ar}), 129.7 (C_{ar}), 128.9 (C_{ar}), 128.8 (C_{ar}), 126.7 (C_{ar}), 125.8 (C_{ar}), 123.6 (C_{ar}), 121.1 (C_{ar}), 119.6 (C_{ar}), 118.7 (C_{ar}), 58.8 ($N\underline{C}H_2C_{ar}$), 54.0 ($N\underline{C}H_2\underline{C}H_2N$), 48.2 ($N\underline{C}H_3$); UV–*vis* (THF): λ_{max} (ε) = 420 nm; HRMS (ESI-TOF) m/z Calcd for $C_{33}H_{30}N_3O_6Ti$ $[M+H]^+$: 612.1609. Found: 612.1612. Anal. Calcd for $C_{33}H_{29}N_3O_6Ti$: 64.82% (C); 4.78% (H), Found: 64.81% (C); 4.80% (H).

Synthetic procedure for **2n**: Following the same procedure as for **2a** with **1n** (300 mg, 0.55 mmol) and Ti(O^iPr)$_4$ (0.16 mL, 0.55 mmol) in 10 mL THF for 15 min. Dipic (92 mg, 0.55 mmol) for 5 h to give **2n** as a red solid (370 mg, 0.49 mmol, 89%). M.p.: 250 °C; IR absorptions (cm^{-1}, ATR): 2955, 2911, 2869, 1684, 1653, 1476, 1342, 1314, 1244, 1181, 1064, 1045, 922, 851, 771, 741; ^{1}H-NMR (600 MHz, $CDCl_3$) δ 9.61 (d, J = 6.0 Hz, 1H, H_{Pyr}), 8.35–8.34 (m, 2H, H_{Pyr}), 8.23–8.22 (m, 1H, H_{pyr}), 7.35 (t, J = 7.8 Hz, 1H, H_{pyr}), 7.04 (t, J = 6.0 Hz, 1H, H_{pyr}), 6.97 (d, J = 12.0 Hz, 4H, H_{ar}), 6.66 (d, J = 6.0 Hz, 1H, H_{pyr}), 5.59 (d, J = 13.2 Hz, 2H, NCH_2C_{ar}), 4.23 (s, 2H, NCH_2Pyr), 3.56 (d, J = 13.2 Hz, 2H, NCH_2C_{ar}), 1.21 (s, 18H, $C(CH_3)_3$), 0.98 (s, 18H, $C(CH_3)_3$); ^{13}C-NMR (151 MHz, $CDCl_3$) δ 169.6 (C=O), 168.1 (C = O), 159.2 (C_{ar}), 157.2 (C_{ar}), 151.1 (C_{ar}), 150.9 (C_{ar}), 149.5 (C_{ar}), 143.8 (C_{ar}), 143.2 (C_{ar}), 138.3 (C_{ar}), 134.7 (C_{ar}), 127.0 (C_{ar}), 126.1 (C_{ar}), 125.4 (C_{ar}), 124.7 (C_{ar}), 123.1 (C_{ar}), 122.5 (C_{ar}), 120.0 (C_{ar}), 65.1 ($N\underline{C}H_2C_{ar}$), 62.7 ($N\underline{C}H_2$), 34.7 ($C_{ar}\underline{C}H_3$), 34.4 ($C_{ar}\underline{C}H_3$), 31.7 ($C(\underline{C}H_3)_3$), 29.7 ($C(\underline{C}H_3)_3$); UV–*vis* (THF): λ_{max} (ε) = 425 nm; HRMS (ESI-TOF) m/z Calcd for $C_{43}H_{54}N_3O_6Ti$ $[M+H]^+$: 756.3487. Found: 756.3521. Anal. Calcd for $C_{43}H_{53}N_3O_6Ti$: 68.34% (C); 7.07% (H), Found: 68.28% (C); 7.11% (H).

Synthetic procedure for **2p**: Following the same procedure as for **2a** with **1p** (300 mg, 0.91 mmol) and Ti(O^iPr)$_4$ (0.22 mL, 0.91 mmol) in 10 mL THF for 15 min. Dipic (167 mg, 1.0 mmol) for 4 h to give **2p** as a red solid (442 mg, 0.82 mmol, 90%). M.p.: 276 °C; IR absorptions (cm^{-1}, ATR): 2982, 2863, 1683, 1657, 1478, 1347, 1312, 1257, 1178, 1069, 978, 924, 853, 774, 741; ^{1}H-NMR (600 MHz, DMSO-d_6) δ 8.57 (t, J = 7.8 Hz, 1H, H_{Pyr}), 8.30 (d, J = 7.8 Hz, 1H, H_{Pyr}), 8.20 (d, J = 9 Hz, 1H, H_{pyr}), 6.89 (s, 2H, H_{ar}), 6.80 (s, 2H, H_{ar}), 4.89 (d, J = 13.8 Hz, 2H, NCH_2), 3.66 (d, J = 13.8 Hz, 2H, CH_2O), 3.17 (t, J = 6 Hz, 2H, NCH_2C_{ar}), 2.93 (t, J = 6 Hz, 2H, NCH_2C_{ar}), 2.18 (s, 6H, $ArCH_3$), 1.78 (s, 6H, $ArCH_3$); ^{13}C-NMR (151 MHz, DMSO-d_6) δ 168.3 (C = O), 167.0 (C=O), 158.0 (C_{ar}), 149.8 (C_{ar}), 148.6 (C_{ar}), 145.6 (C_{ar}), 130.2 (C_{ar}), 128.8 (C_{ar}), 128.0 (C_{ar}), 126.5 (C_{ar}), 126.1 (C_{ar}), 125.7 (C_{ar}), 122.5 (C_{ar}), 62.6 ($N\underline{C}H_2C_{ar}$), 56.1 ($N\underline{C}H_2CH_2$), 53.4 ($NCH_2\underline{C}H_2$), 21.0 ($C_{ar}\underline{C}H_3$), 15.4 ($C_{ar}\underline{C}H_3$); UV–*vis* (THF): λ_{max} (ε) = 411 nm; HRMS (ESI-TOF) m/z Calcd for $C_{27}H_{28}N_2O_7Ti$ $[M+H]^+$: 540.3945. Found: 540.3925. Anal. Calcd for $C_{27}H_{27}N_2O_7Ti$: 60.12% (C); 5.05% (H), Found: 60.22% (C); 5.15% (H).

MTT assay

Cells were cultivated at 37 °C in humidified 5% CO_2 atmosphere using Dulbecco's DMEM-media (Invitrogen) containing 10% foetal calf serum, 1% penicillin and 1% streptomycin. Cells were split every three days. Both cell lines were tested on mycoplasma infections using a mycoplasma detection kit (Shanghai Jingkang Biological Engineering Co., Ltd.). Cells were seeded into a 96-well plate (Hela S3 cells, Hep G2 cells and AML 12 cells were seeded with 5000 cells/well), and the cells were placed in an incubator with 5% CO_2 atmosphere at a constant temperature of 37 °C for 24 h to allow the cells to grow adherently. Different concentrations of Ti(IV) complexes were added to each well. Complexes were dissolved and diluted with dimethyl sulfoxide (DMSO) to prepare solutions of different concentrations (10^{-1}, 10^{-2}, 10^{-3}, 10^{-4}, 10^{-5}, 10^{-6} and 10^{-7} mol/mL). One portion of dimethyl sulfoxide solution of complex was added to 99 portions of DMEM medium with 10% fetal bovine serum (FBS), making the final solution content in each well to be 100 µL, and was then incubated for 48 h. After 48 h, 10 µL of MTT solution at a concentration of 5 mg/ mL was added to each well and the plates were incubated for 4 h. After incubation, aspirate the solution from each well, 100 µL sterile DMSO solution was added to the wells and was shaken for ten minutes, and use enzyme-linked immune-assay the detector is tested at a wavelength of 562 nm. In the experiment, zero adjustment wells (medium, MTT solution and DMSO solution) and control wells (non-administered group) were both set up. Five parallel controls were set for each concentration gradient to avoid experimental errors. Each experiment was repeated three times. The statistical weights of repeated experiments are the same; the IC_{50} value for each complex is the average value of three independent experiments. The error value of the IC_{50} value is calculated from the standard deviation. The resulting curves were fitted using Sigma plot 10.0 [31]. The detailed sigmoidal plots of each complex are depicted in the SI (Figure S6 and S7), where all test compounds show fully converged sigmoidal curves.

Flow cytometric analysis

Tumor cell death induced by **2j**, **2n** and **2p** were quantified by flow cytometry using the Annexin V-FITC/PI Assay kit (Biosharp BL110A) in accordance with the manufacturer's protocol. Hela S3 cells were seeded in a 6-well plate at a density of 1×10^6 cells per well and allowed to settle for 24 h. The medium was replaced with fresh one containing complex **2j**, **2n** and **2p** with final concentrations of 10^{-2} µM, 1 µM and 10^2 µM, respectively. After incubation for 24 h, the cells were trypsinized, centrifuged (1000 rpm, 5 min) and washed 2 times with cold PBS. Fresh cells were collected and resuspended in 250 µL of binding buffer, stained with 5 µL of Annexin-V-FITC and 10 µL of PI. Finally, the samples were analyzed by BD Accuri™ C6 Plus flow cytometer. The cellular density plots were obtained by FlowJo 7.2.5 [32].

Cellular uptake of titanium

Hela S3 cells were seeded in a 6-well plate at a density of 2×10^5 cells per well and incubated for 24 h, the cells were treated with **2j**, **2n**, **2p** and **[(Salan$^{2,4-Me}$)Ti(IV) Dipic]** (2 µM) for 10 min, 30 min, 1 h, 2 h, 24 h and 48 h, respectively. Each experiment was repeated three times. The attached cells were harvested with trypsin and washed twice with PBS (4 °C). Cell pellets were collected by centrifugation and then were digested with nitric acid (100 µL) for 2 h at 95 °C, followed by reacting with H_2O_2 (50 µL) at 95 °C for 1.5 h. 100 µL of hydrochloride acid (38%) was added to the mixture, which was then kept at 95 °C open to air till the total volume was less than 50 µL, H_2O was added to dilute the residue to 5 mL, from which a sample was taken and subjected to ICP-MS analysis for titanium content. Control group: Following the same experimental procedures using Hela S3 cells without treatment of **2j**, **2n**, **2p** and **[(Salan$^{2,4-Me}$)Ti(IV)Dipic]**, no titanium was detected by ICP-MS (0 ng).

ROS detection

ROS levels in Hela S3 cells were detected with H_2DCFDA probe [33]. Hela S3 cells were seeded in a 12-well plate (6×10^4 cells per well) with round coverslips placed in each well, then the cells were incubated in 5% CO_2 atmosphere at 37 °C for 24 h. Four wells with the cell densities reached to 30%-50% were selected and to which each 2 µM of **2j**, **2n**, **2p** and **[(Salan$^{2,4-Me}$)Ti(IV)Dipic]** (in DMEM medium with 10% FBS) were administrated, respectively. The cells were further incubated for another 24 h under the same condition above. The solution of the four wells was aspirated and washed with PBS, then stained with 10 µM H_2DCFDA and incubated for 30 min at 37 °C in an incubator protected from light. The cells were then washed 2 times with DMEM medium (serum-free) to fully remove H_2DCFDA that had not entered the cells. Transfer each coverslip to a glass slide and fluorescence imaging (DCF, oxidized form of H_2DCFDA) was conducted by fluorescence microscopy.

Results and discussion

In this study we focused on three different types of *bis*-chelates, i.e. Dipic stabilized Salans **2a**-**2 l** ([ONNO]-type), backbone functionalized **2m**-**2o** ([ONON]-type) and **2p**-**2r**

([ONOO]-type). Salan ligands were synthesized by Mannich reaction of ethylenediamine (**1a**-**1 l**), 2-picolylamine (**1m**-**1o**) or *N*-(2-hydroxyethyl)amine (**1p**-**1t**) (see Scheme 2) [10, 34]. The ligands were metalated smoothly by reaction with equimolar amounts of $Ti(O^iPr)_4$ in THF for 15 min followed by addition of 1.1 equiv. of Dipic for 3–6 h to give the final *bis*-chelates **2** [23]. The compound library comprises 10 different [ONNO] type Ti(IV) complexes **2a**-**2j** with unsubstituted Dipic as the second chelator and two complexes **2 k** and **2 l** with substituted Dipic. Three *bis*-chelates **2m**-**2o** from the 2-picolylamine substituted [ONON] type ligand as well as three members of the *N*-(2-hydroxyethyl)amine substituted [ONOO] type **(2p**-**2r)** completed the library. After complete consumption of the ligands **1s** and **1t** during metalation, only unidentifiable precipitates were isolated. Results are summarized in Scheme 2 and Table 1, detailed synthetic procedures and compound characterization can be found in the SI.

Solid-state molecular structure

Suitable crystals for X-ray diffraction analysis of **2f**, **2h** and **2q** were obtained by slow diffusion of *n*-hexane to a saturated CH_2Cl_2 solution of each complex at r.t.. Crystals of **2n** were obtained by diffusion of *n*-hexane to a solution of **2n** in a mixture of CH_2Cl_2 and MeOH (10:1 = *v*/*v*) at r.t.. All four solid-state molecular structures are presented in Fig. 1. **2f** and **2n** crystalized in the triclinic space group P-1. **2f** is accompanied by one CH_2Cl_2 molecule and **2n** is accompanied by two MeOH molecules. **2h** and **2q** crystalized in monoclinic space group $P2_1/c$, and **2h** is accompanied by 3/4 MeOH molecule. **2f** and **2h** are C_2 symmetric while **2n** and **2q** are C_s symmetric in their solid-states, respectively. Selected bond lengths and angles are summarized in Table 2. Both Salan complexes **2f** and **2h** have a pentagonal-bipyramidal geometry like their ancestor **([(Salan$^{2,4-Me}$)Ti(IV)Dipic])** [20] with two notable exceptions. First, the Dipic in **2f** is located closer to the Ti compared to both, **2h** and the ancestor complex, as indicated by the shorter Ti–O(3/4) (2.03, 2.04 Å) and Ti-N(3) (2.17 Å) distances. Second, the O(1)–Ti–O(2) angle is more linear in **2f** and **2h** (172.2, 171.9°) compared to **([(Salan$^{2,4-Me}$)Ti(IV)Dipic])** (168.9°). However, the O(1)–Ti–O(2) angle of [ONON]-type **2n** and [ONOO]-type **2q** (165.1° and 166.0°) are even smaller, i.e. more bend, than in the **([(Salan$^{2,4-Me}$)Ti(IV)Dipic])**. Moreover, the dihedral angle of the phenyl plains in **2n** and **2q** (145.6° and 155.2°) are much bigger compared to **2f**, **2h** and **([(Salan$^{2,4-Me}$)Ti(IV)Dipic])** (102.4°, 109.5° and 110.5°). The above findings let the Ti(IV) centers of **2n** and **2q** appear more exposed than those in the [ONNO]-type Ti(IV) complexes.

Next, we focused on the distances of the Ti(IV)-center from the heteroatoms of both the core ligand (N(1)) and the distant 'arm' of complexes **2n** (N(2)) and **2q** (O(7)). Therefore, **2n** was compared with structurally related Dipic *bis*-chelates **Ti-1**– **Ti-4** [23, 35, 36] and **Ti-5** [37] and **2q** was compared with the Titanatranes **Ti-6** [38] and **Ti-7** [39] (Fig. 2). The Ti–N(1) distance of **2n** (2.35 Å) does not significantly differ from its peers (2.33–2.37 Å) (Table 3). However, the Ti–N(2) distance is more sensitive to the type of amine used in the side 'arm', i.e., for the NMe_2- 'arm' the Ti–N(2) distance is longer (2.39–2.41 Å) than for the pyridyl-arm in **2n** (2.37 Å) and **Ti-5** (2.29 Å) [40, 41]. For **2n**, this is a direct consequence of the lower steric requirements of the pyridyl ligand compared to the aliphatic amine in **Ti-1**–**Ti-4**, but in **Ti-5** this effect is enhanced by the change in ligand sphere (Dipic *vs* non-chelating isopropoxide). In **2q**, the distance of the Ti(IV) to the oxygenated 'arm' O(7) is almost 0.4 Å larger than in the comparable titanatrane **Ti-6** [38]. This is because the chelating amino-*bis*-phenolate **1q** in combination with the dianionic tridentate Dipic is sufficient to compensate for the charge of the Ti(IV). Indeed, we were able to localize the alcohol proton in the diffraction data, which explains the rather lose association of O(7) to the Ti(IV). A similar binding situation is found in the dimeric μ-oxo bridged *O*-methylated titanatrane **Ti-7** with a Ti–OMe distance of 2.31 Å [39]. The other Ti–O distances (Ti–O(1/2) and Ti–O(3/4)) remain fairly unaffected and were found in the range of other *bis*-chelates. The detailed values are summarized in Table 3 [42].

Stability and hydrolysis

It is known from previous reports that the aqueous stability and antitumor activity of phenolato Ti(IV) complexes are significantly influenced by the substituents at the phenolato *ortho*-position [21]. The Ti(IV) *bis*-chelates bearing less sterically demanding substituents such as methyl at this position remained stable in aqueous media and even on silica gel. At the same time they were highly toxic to tumor cells [20] but hydrolysable when presented to extreme conditions (pH = 1.9 and 12.1) [21]. In contrast, Ti(IV) complexes bearing bulky substituents such as *t*-butyl at the phenolato *ortho*-postion, were stable over the impressive pH-range of 1.9–12.1. However, they were also completely biological inactive. We attributed this to the over protection of the Ti(IV) center, which renders the corresponding Ti(IV) complexes kinetically inert and thus unable to react with a cellular target [21]. With these findings in mind, we investigated the hydrolysis of representative Ti(IV) Salan-complexes ([ONNO]-type) **2e**-**2 k**, the [ONON]-type complexes **2m**-**2o** as well as the [ONOO]-type complexes **2q**-**2r**.

All selected Ti(IV) complexes were subjected to 1×10^5 equiv. of H_2O and the reaction progress monitored by time-resolved UV–*vis* spectroscopy [21]. Results are summarized in Table 4. The following trends were observed:

[ONNO]-type complexes with unsubstituted Dipic and no *ortho*-substituents at the phenol hydrolyzed with $t_{1/2}$ of 46 – 97 h (**2e**, **2g**-**2i**) much faster than the *ortho*-substituted counterpart **2f** which proofed stable during the observation time [21, 43]. From this group, the donor-substituted complexes (**2g**, **2h**) resist hydrolysis twice as long as their competitors (**2e**, **2i**) which we attribute to a diminished electrophilicity at the Ti(IV) center. *β*-Naphthol based Salan complexes had a $t_{1/2}$ of less than 30 h, regardless of the second chelating agents, i.e. Dipic (**2j**) or 4-hydroxy-Dipic (**2k**). The lack of *ortho*-substitution at the naphthol further attributes to the diminished aqueous stability of these *bis*-chelates.

The hydrolysis of the [ONON]-type complexes **2m**-**2o** underlines the above results, as only the *ortho*-substituted complex **2n** remained stable under the studied regime, whereas the other two *ortho*-unsubstituted complexes **2m** and **2o** hydrolyzed with $t_{1/2}$ of 20–23 h. Obviously, the picolylamine side arm does not lead to additional stability [14]; On the contrary, compared to **2e**, the Salan with the same substitution pattern at the phenol, the half-live of **2o** is more than halved. This is an indication for a weakened ligand sphere where the remote donor at the side arm acts as a predetermined breaking point [40, 41]. The [ONOO]-type **2p**-**2r** and the only [ONON]-type complex **2n**, bearing *ortho*-alkyl substitutions such as methyl or *t*-butyl on the phenolato ligands all remained stable. (SI, Figure S8-S20). Hence, we conclude that the aqueous stability of [ONON] and [ONOO] type Ti(IV) complexes is primarily influenced by the substituents on the phenolato *ortho*-position; which is similar to the Salan type Ti(IV) complexes.

In addition, we have examined the aqueous stability of **2o** and **2p** in DMEM/F12 cell media [26]. However, results indicate that there is no significant difference compared to the hydrolysis in pure water (SI, Figure S21). Furthermore, hydrolysis of **2n**, **2r** and a reported **[(Salan$^{2,4-t\mathrm{Bu}}$)Ti(IV) Dipic]** in a buffer solution (pH = 2.92) was performed aiming to access a direct comparison of their aqueous stability. The $t_{1/2}$ of **2n** and **2r** were 8 h and 9 h, and **[(Salan$^{2,4-t\mathrm{Bu}}$)Ti(IV) Dipic]** was stable during the observation time (2 weeks). Previous studies identified the sole hydrolysis products for Salan Ti(IV) *bis*-chelates as Salan ligands, accompanied by small amounts of insoluble precipitates, which could be TiO_2 partially complexed by Dipic [23]. Hence, the products of hydrolysis of **2j**, **2o** and **2p** from scaled-up reactions were isolated and characterized [23]. As anticipated, ligands **1j**, **1o** and **1p** were detected by HRMS (High resolution mass spectrometry) and ^{1}H-NMR. For detailed experimental procedures, refer to SI, Figure S25-S30.

Cytotoxicity assay

Cytotoxicity of all phenolato Ti(IV) *bis*-chelates was determined on Hela S3 (Human cervical carcinoma) and Hep G2 (Human derived hepatoma) cells by MTT assay (Methylthiazolyldiphenyl-*tetra*-zolium bromide) with cisplatin used as a reference. The IC_{50} value of each Ti(IV) complex was derived from the average of the data from three experiments at different days, and in each repeat, all concentrations were repeated for five times. The error values were obtained by standard deviation of all experiments. As depicted in Table 5, **2a** and **2b** with halogens (Cl and F) on the 2 and 4-positions of Salan demonstrated comparable antitumor activity to cisplatin (Entries 1–2). In comparison with **2d** (Salan$^{2-\mathrm{Methyl},4-\mathrm{Cl}}$), **2c** (Salan$^{4-\mathrm{Cl}}$) showed decreased inhibition activity on Hela S3 cells (Entries 3–4). Whereas the inhibition activity against Hep G2 cells of **2e** and **2f** with Br in the 2 and 4-position (Salan) vanished (Entries 5–6). Methoxy, 1,3-dioxolanyl and 4-phenyl functionalized Salans **2g**, **2h** and **2i** had slightly decreased inhibitory activity against both cell lines compared to **2a** and **2b** (Entries 7–9). Naphthalenyl **2j** exhibited the lowest IC_{50} values against both cells in the [ONNO] series; Modification on the Dipic in position 4 with a hydroxyl (**2k**) or a chlorine (**2l**) either had negative or no influence on the inhibition activity (Entries 11–12); [ONON] type **2m**, **2n** and **2o** all demonstrated excellent antitumor activity against Hela S3 cells with no influence from *t*-butyl on phenolato 2-position. (Entries 13–15). Similar to **2e** and **2f**, Br also led to decreased activity of **2o** against Hep G2 cells. [ONOO] type **2p**, even **2q** and **2r** bearing *t*-butyl at the 2 or 4-position all showed potent anti-tumor activity (Entries 16–18). The three most potent complexes **2j**, **2n** and **2p** were then examined for their cytotoxicity against healthy AML12 cells (Alpha mouse liver 12). While **2j** and **2p** exhibited modest activity, **2n** was completely inactive with a maximum inhibition rate reaching 58% (See SI, Figure S7). Additionally, ligands **1j**, **1n** and **1p** were found to show significantly reduced or almost none inhibitory activity in Hela S3 and Hep G2 cells (See SI, Figure S6, bottom row).

The structure–activity relationship of these phenolato Ti(IV) *bis*-chelates is shown in Fig. 3. Halogens such as Fluorine and Chlorine can enhance the cytotoxicity; Bromine does decrease the cytotoxicity against Hep G2 cells; Substitutions on the phenolato 2-position are essential for maintaining aqueous stability and methyl group increase cytotoxicity against Hep G2 cells; Bulky substituents on the 2-position lead to a complete loss of cytotoxicity; Electron donating alkoxyl groups can decrease cytotoxicity; Naphthalenyl ligand can enhance the cytotoxicity probably due to the enhanced aromatic system facilitating the cellular uptake or DNA interaction [44]; The introduction of a hydroxyl group on position 4 of the Dipic decreased the antitumor activity probably due to an enhanced dipole moment. 2-Picolylamine bearing Ti(IV) complexes generally showed good inhibition activity against Hela S3 cells even with steric demanding groups on the phenolato 2-position.

Even bromine in position 2 only slightly decreased the activity against Hep G2 cells. Ti(IV) complexes containing the *N*-(2-hydroxyethyl) group in their backbones are potent cytotoxic agents with also almost no influence from the bulky groups at 2-position. In a previous study a naphthalenyl based [ONON] type Ti(IV) complex was completely inactive against Hela S3 and Hep G2 cells. The complex regained significant cytotoxicity only after the introduction of OH to the 4-position of Dipic [23]. This is in contrast to our results for the [ONNO] type **2j**, which is itself highly active and loses its cytotoxicity when Dipic is replaced by Dipic^{4-OH}.

Apoptosis assay

Apoptotic cell death is preferred over necrosis because the former is a programmed cell death path, and significantly reduces side effects and inflammations during anti-cancer treatment [45]. The three most cytotoxic complexes **2j**, **2n** and **2p** were selected for apoptosis analysis on Hela S3 cells using the Annexin V-FITC/PI apoptosis assay kit. Hela S3 cells were treated with 1 µM, 10 µM and 100 µM of Ti(IV) complexes for 48 h and were analyzed with the BD Accuri™ C6 Plus flow cytometer. The cellular density plots were visualized by FlowJo 7.2.5. The experiment was repeated for three times, and the representative experiments are depicted in Fig. 4, **2j** induced 25.9%, 49.2% and 87.6% of apoptotic cells at the three concentrations, respectively. **2n** (**2p**) led to 21.9% (19.6%) at the lowest, 42.2% (41.1%) at the middle and 83.1% (75.9%) apoptosis of Hela S3 cells at the highest concentration. This suggests that the trigger of apoptosis is more pronounced with increased concentration of the Ti(IV) complexes. The maximum amount of necrotic cells induced by **2j**, **2n** and **2p** are 0.72%, 2.70% and 3.74% at 100 µM (Control: 0.24%, 0.27% and 0.43%). At the concentration of 100 µM, the percentage of apoptotic Hela S3 cells of dead cells for **2j**, **2n** and **2p** are 99.2%, 96.9% and

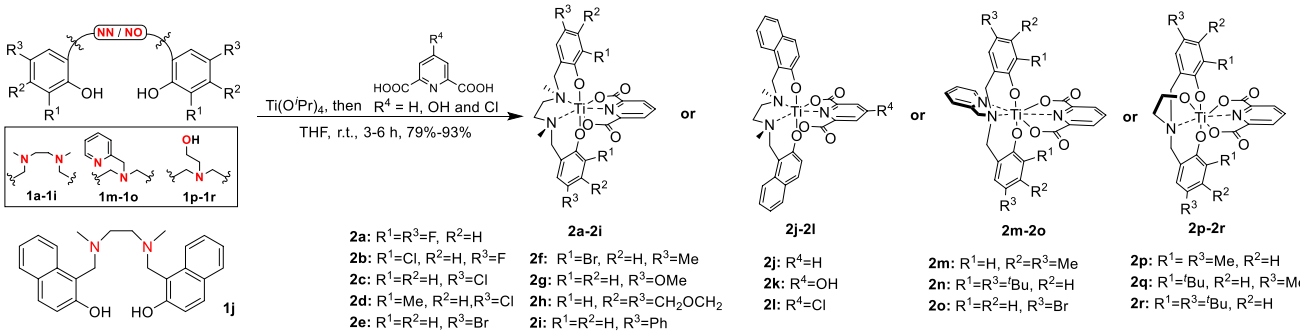

Scheme 2. Synthesis of [ONNO] (**2a**-**2l**), [ONON] (**2m**-**2o**) and [ONOO] type (**2p**-**2r**) amino-*bis*(phenolato) Ti(IV) complexes

Table 1 Results of the synthesis of [ONNO], [ONON] and [ONOO] type phenolato Ti(IV) complexes stabilized by Dipic (2,6-dipicolinic acid)

Entry[a]	Ligand[b]		Time (h)	Product	Yield[c] (%)	Entry[a]	Ligand[b]		Time (h)	Product	Yield[c] (%)
1	**1a**	$R^1=R^3=F$, $R^2=H$	6	**2a**	93	11	**1k**	$R^4=OH$	3	**2k**	80
2	**1b**	$R^1=Cl$, $R^2=H$, $R^3=F$	5	**2b**	85	12	**1l**	$R^4=Cl$	4	**2l**	80
3	**1c**	$R^1=R^2=H$, $R^3=Cl$	3	**2c**	80	13	**1m**	$R^1=H$, $R^2=R^3=Me$	5	**2m**	89
4	**1d**	$R^1=Me$, $R^2=H$, $R^3=Cl$	6	**2d**	90	14	**1n**	$R^1=R^3={}^tBu$, $R^2=H$	5	**2n**	88
5	**1e**	$R^1=R^2=H$, $R^3=Br$	5	**2e**	81	15	**1o**	$R^1=R^2=H$, $R^3=Br$	5	**2o**	80
6	**1f**	$R^1=Br$, $R^2=H$, $R^3=Me$	4	**2f**	82	16	**1p**	$R^1=R^3=Me$, $R^2=H$	4	**2p**	90
7	**1g**	$R^1=H$, $R^2=H$, $R^3=OMe$	4	**2g**	79	17	**1q**	$R^1={}^tBu$, $R^2=H$, $R^3=Me$	5	**2q**	85
8	**1h**	$R^1=H$, $R^2=R^3=CH_2OCH_2$	5	**2h**	82	18	**1r**	$R^1=R^3={}^tBu$, $R^2=H$	5	**2r**	88
9	**1i**	$R^1=R^2=H$, $R^3=Ph$	4	**2i**	91	19	**1s**	$R^1=R^3=Cl$, $R^2=H$	48	**2s**	0[d]
10	**1j**	$R^4=H$	3	**2j**	93	20	**1t**	$R^1=Me$, $R^2=H$, $R^3=F$	48	**2t**	0[d]

[a]Reaction was carried out at r.t. without N_2 protection using amino-*bis*(phenolato) ligands **1a**-**1t** (0.84 mmol, 1.0 equiv.), $Ti(O^iPr)_4$ (0.84 mmol, 1.0 equiv.) and Dipic (0.92 mmol, 1.1 equiv.) in 10 mL of THF. [b] R^1, R^2 and R^3 are substituents on amino-*bis*(phenolato) ligands and R^4 is the substituent on 4-position of Dipic. [c] Isolated yield. [d] Quant. consumption of starting material

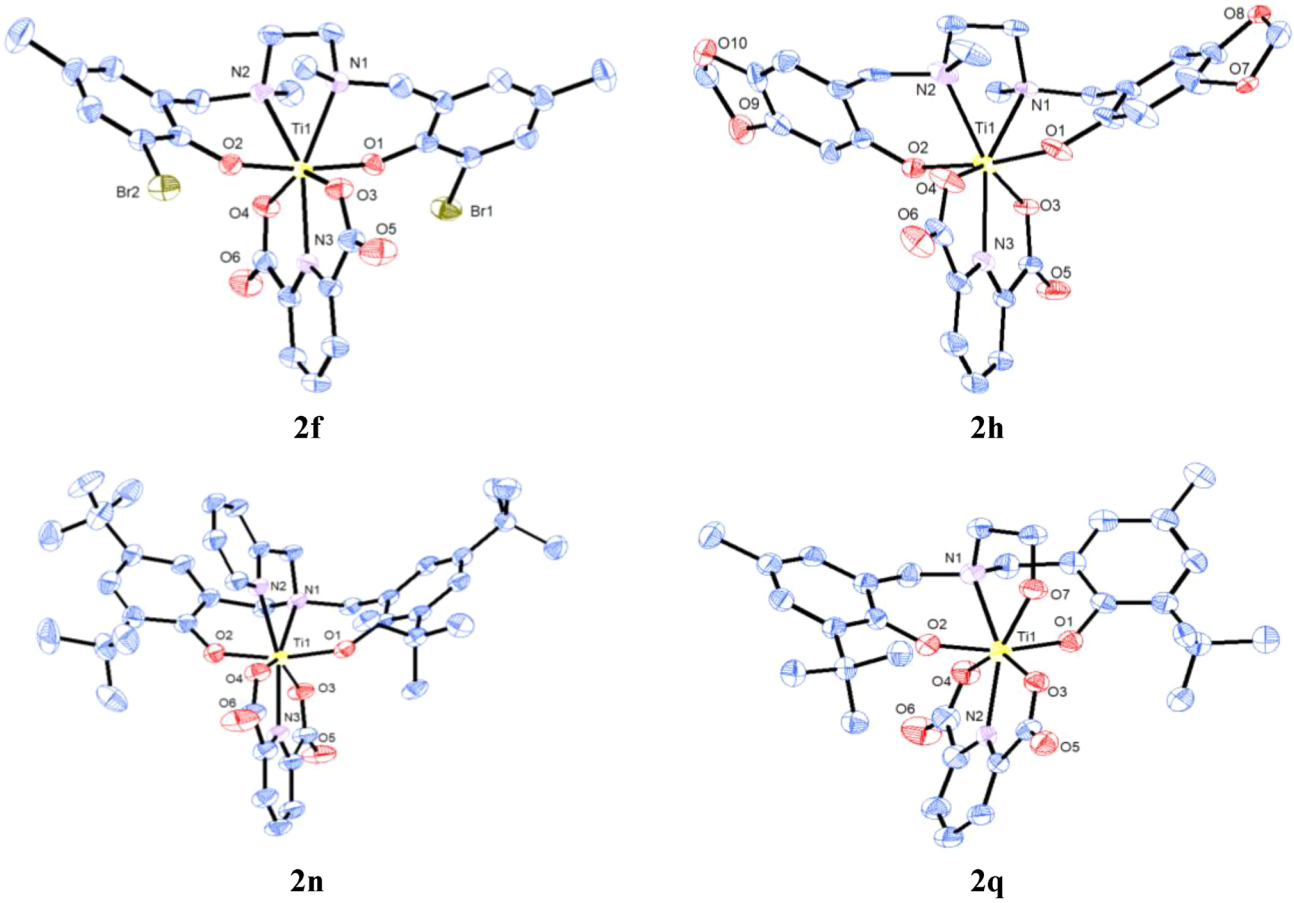

Fig. 1 Solid state molecular structures of approximate C_2 symmetric heptacoordinated heteroleptic **2f** and **2h** and C_s symmetric heptacoordinated heteroleptic **2n** and **2q**. Thermal ellipsoids are drawn at the 50% probability level. Hydrogen atoms and solvent molecules are omitted for clarity

95.3%, respectively. This is a good indication that apoptosis is indeed almost exclusively induced.

Cellular uptake

Cellular uptake of **([(Salan$^{2,4-Me}$)Ti(IV)Dipic])**, **2j**, **2n** and **2p** by Hela S3 cells was investigated by ICP-MS (Inductively coupled plasma mass spectrometry). Each Ti(IV) complex (4×10^{-9} mol, total titanium: 191 ng) of **([(Salan$^{2,4-Me}$)Ti(IV)Dipic])**, **2j**, **2n** and **2p** was administered to the cells, and the cell samples for every Ti(IV) complex were incubated for 10 min, 30 min, 1 h, 2 h, 24 h and 48 h, respectively. 3 parallel experiments were set for each Ti(IV) complex at all time points. The uptake amounts of titanium were depicted in average values with errors calculated by standard deviation (Table S6, SI). The percentages of titanium found in the cells with respect to the total amount of titanium added was used to calculate the ability of cellular titanium uptake. As depicted in Fig. 5, the titanium uptake of **([(Salan$^{2,4-Me}$)Ti(IV)Dipic])** by Hela S3 cells at 10 min

Table 2 Selected bond lengths (Å) and angles (deg) for **2f**, **2h**, **2n**, **2q** with **([(Salan$^{2,4-Me}$)Ti(IV)Dipic])** from ref. [20] for comparison

	2f	2h	2n	2q	[(Salan$^{2,4-Me}$)Ti(IV)Dipic]
O(1)-Ti	1.853(18)	1.860(2)	1.848(2)	1.831(3)	1.850(13)
O(2)-Ti	1.847(18)	1.837(2)	1.838(2)	1.836(3)	1.844(12)
O(3)-Ti	2.029(18)	2.048(2)	2.064(2)	2.067(3)	2.043(13)
O(4)-Ti	2.040(18)	2.057(2)	2.032(2)	2.046(3)	2.046(12)
N(1)-Ti	2.373(2)	2.359(3)	2.351(2)	2.322(4)	2.350(15)
N(2)-Ti	2.381(2)	2.379(2)	2.366(3)	2.179(4)	2.384(15)
N(3)-Ti	2.167(2)	2.186(2)	2.209(3)	2.209(3)[a]	2.185(14)
O(1)-Ti–O(2)	172.18(8)	171.89(9)	165.09(9)	165.98(14)	168.92(5)
O(3)-Ti–O(4)	142.94(7)	142.34(9)	140.62(9)	141.90(13)	141.37(5)
N(1)-Ti-N(2)	73.21(7)	73.44(9)	71.67(9)	72.72(12)[b]	73.48(5)

[a]Ti–O(7). [b] N(1)-Ti–O(7)

was 8.5%. The uptake then slowly increased over time to 8.7%, 9.0%, 9.2%, 9.4% and 9.5% after 30 min, 1 h, 2 h, 24 h and 48 h, respectively. This implies a fast cellular uptake process of **[(Salan$^{2,4-Me}$)Ti(IV)Dipic]**, since already 90% of the maximum titanium uptake (value after 48 h, 18.1 ng) was achieved within 10 min. The absolute cellular uptake of **2j** is slightly higher with 14.9%, 15.2%, 15.4%, 15.7%, 15.9% and 16.0% after the same sampling interval. Hence, in total 93% of maximum titanium uptake (titanium uptake at 48 h, 30.6 ng) was already reached within 10 min. While the absolute titanium uptake of **2n** is lower, the percentages at different time were 7.9%, 8.3%, 8.5%, 8.7%, 8.8% and 8.8%, resulting in 89% of the maximum titanium uptake (48 h, 16.9 ng) after 10 min. The uptake rate of **2p** was comparable to **2n** with uptake percentages to be 8.4%, 8.6%, 8.7%, 8.9%, 9.1% and 9.2% at testing points, and 91% of the maximum titanium uptake reached after 10 min. All phenolato Ti(IV) *bis*-chelates exhibited rapid cellular uptake, with approximately 90% of the maximum uptake (after 48 h) being reached within 10 min [23]. The expanded aromatic system in the *β*-Naphthol derived **2j** can obviously facilitate the cellular uptake and led to enhanced antitumor activity.

Intracellular ROS assessments

The generation of ROS can trigger oxidative stress and is associated with several cellular targets, such as single-strand DNA breakage, mitochondrial membrane destruction, lipid peroxidation and destruction of secondary protein structures, thus procedural cell death can be induced such as apoptosis, autophagy, necroptosis or ferroptosis [46]. We have investigated the ROS generation of representative complexes **2j**, **2n**, **2p** and **[(Salan$^{2,4-Me}$)Ti(IV)Dipic]**. The H_2DCFDA probe was employed for ROS detection. H_2DCFDA has no intrinsic fluorescence, but after reacting with ROS, the formed fluorescent DCF can be detected by fluorescence microscopy [33]. The experiment was repeated for three times. As shown in Fig. 6 (representative experiments), ROS generation was detected with all four Ti(IV) complexes, among them, **2j** showed the highest level of induced ROS, which was slightly higher than the ROS from **[(Salan$^{2,4-Me}$)Ti(IV)Dipic]**. In direct comparison, the ROS level generated by **2n** and **2p** was significantly reduced. Tshuva *et.al* reported recently that a PhenolaTi complex could induce tumor cell death via ER (endoplasmic reticulum) stress,

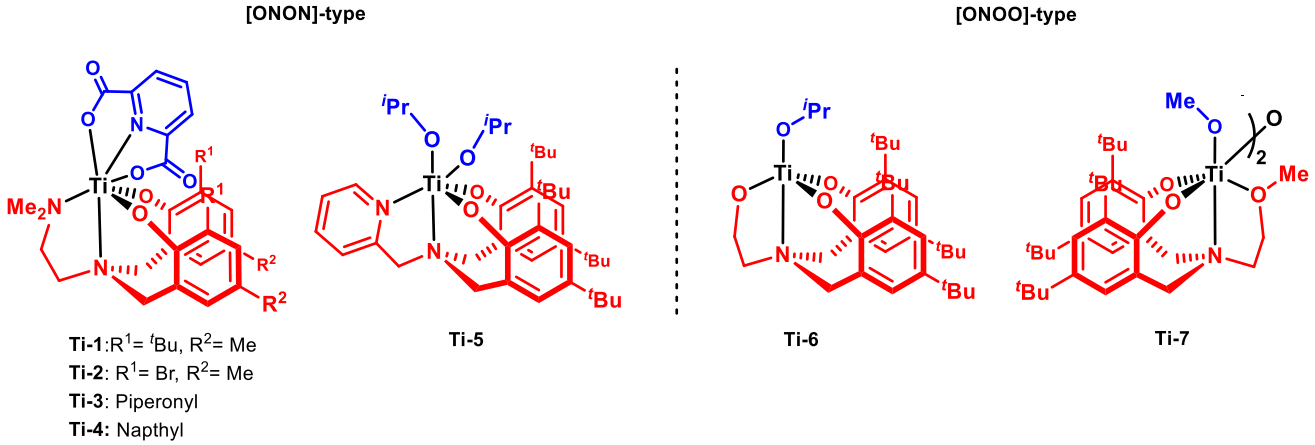

Fig. 2 Graphical representation of [ONON]-type complexes **Ti-1** – **Ti-5** and [ONOO]-type complexes **Ti-6** and **Ti-7**. Core ligands are depicted in red [42]

Table 3 Ti(IV) – heteroatom distances of both the core ligand and the distant 'arm' of complexes **2n**, **2q** and the structurally related comparison group of **Ti-1** – **Ti-7**

	[ONON]-type						[ONOO]-type		
	2n	**Ti-1**[b]	**Ti-2**	**Ti-3**	**Ti-4**	**Ti-5**	**2q**	**Ti-6**	**Ti-7**
Ti-N[a] (Core ligand)	2.35	2.34	2.36	2.37	2.33	2.34	2.32	2.33	2.29
Ti-N (Side arm)	2.37	2.41	2.39	2.40	2.39	2.29	/	/	/
Ti–O (Core ligand)	1.85 1.84	1.84 1.83	1.86 1.84	1.83 1.84	1.84 1.84	1.92 1.90	1.83 1.84	1.84 1.85	1.88 1.89
Ti–O (Side arm)	/	/	/	/	/	/	2.21	1.83	2.30 2.32

[a] All distances in Å; [b] CSD-Mercury accession codes are: **Ti-1**: ECUHUJ; **Ti-2**: ECUHIX; **Ti-3**: HAVDIV; **Ti-4**: UBICAN; **Ti-5**: DEVFIU; **Ti-6**: PICGAK; **Ti-7**: NUPQOH

Table 4 Half-Lives ($t_{1/2}$) of representative Ti(IV) complexes in 1/5 mixture (*v/v*) of H_2O/THF

Entry[a]	Complex	$t_{1/2}$ (h)	λ_{max} (nm)[c]
1	**2e**	46	386
2	**2f**	stable[b]	401
3	**2g**	95	425
4	**2h**	97	444
5	**2i**	55	416
6	**2j**	26	420
7	**2k**	30	426
8	**2m**	23	423
9	**2n**	stable[b]	432
10	**2o**	20	418
11	**2p**	stable[b]	415
12	**2q**	stable[b]	417
13	**2r**	stable[b]	419

[a]Hydrolysis was followed by time-resolved UV–*vis* spectroscopy after mixing 2.5 mL THF solution of Ti(IV) complex (5.6×10^{-6} mmol/L) with 0.5 mL of H_2O (1×10^5 equiv.) at 37 °C. [b] No decomposition after 2 weeks. [c] λ_{max} of each Ti(IV) complex was determined by UV–*vis* spectroscopy

leading to hypoxia and mitochondrial ROS [47]. Hence, the role of ROS of the Ti(IV) complexes in this study with respect to the induced apoptotic cell death requires further evidence.

Conclusion

In summary, we have synthesized three types of amino-*bis*(phenolato) Ti(IV) complexes stabilized by 2,6-dipicolinic acid as a second chelator. These comprise Salan Ti(IV) *bis*-chelates with a diversified substitution pattern, i.e. two novel types of Ti(IV) *bis*-chelates containing 2-picolylamine and *N*-(2-hydroxyethyl) in the amino-phenolato backbone. All Ti(IV) complexes have good to excellent aqueous stability, and release the amino-*bis*(phenolato) ligands as the sole products of hydrolysis. In contrast to the [ONNO] type Ti(IV) complexes, the [ONON] type (2-picolylamino) and [ONOO] type (*N*-(2-hydroxyethyl)) Ti(IV) complexes were hydrolyzable even with bulky substituents at position 2 of the phenolato ligands. We explain this by a more accessible Ti(IV) center of the [ONON] and [ONOO] type complexes as evident from the solid-state molecular structures. Most of the Ti(IV) complexes have potent inhibitory activity against Hela S3 and Hep G2 cells. Preliminary investigation of **2p**, **2j** and **2n** on AML12 cells revealed that their cytotoxicity against primary cell lines is significantly reduced or even disappears completely. Based on these findings we drafted a preliminary structure–activity relationship with respect to different substitution pattern on the ligand system. Moreover, the three most potent Ti(IV) complexes, **2p**, **2j** and **2n**, were shown to exhibit rapid cellular uptake and to induce almost exclusively apoptosis of Hela S3 cells. The highest induced apoptosis level of **2j** may be related to its higher induced ROS generation compared to **2p** and **2n.** In summary, these eighteen novel phenolato Ti(IV) *bis*-chelates do not only expand the library of group 4 antitumor metal complexes, but also lead to several highly potent Ti(IV) complexes. The

Table 5 IC_{50} values obtained via MTT assay against Hep G2, Hela S3 and AML12 cells

Entry	Complex	Hep G2[a] IC_{50} [μM]	Hela S3[a] IC_{50} [μM]	Entry	Complex	Hep G2[a] IC_{50} [μM]	Hela S3[a] IC_{50} [μM]
1	**2a**	2.3 ± 0.7	4.8 ± 1.4	12	**2l**	10.3 ± 1.7	1.0 ± 0.3
2	**2b**	2.1 ± 0.5	1.7 ± 0.6	13	**2m**	15.4 ± 1.7	1.0 ± 0.2
3	**2c**	45.6 ± 15.1	1.7 ± 0.3	14	**2n**[c]	**4.3 ± 1.1**	**0.2 ± 0.1**
4	**2d**	1.3 ± 0.5	11.1 ± 3.6	15	**2o**	39.9 ± 12.3	0.8 ± 0.1
5	**2e**	228.6 ± 92.6	9.7 ± 3.1	16	**2p**[b]	**10.4 ± 1.5**	**0.2 ± 0.1**
6	**2f**	191.2 ± 62.9	4.8 ± 0.9	17	**2q**	6.9 ± 0.8	1.3 ± 0.5
7	**2g**	25.4 ± 9.5	15.8 ± 4.3	18	**2r**	18.3 ± 4.4	11.6 ± 3.4
8	**2h**	17.9 ± 6.0	19.0 ± 6.7	19	**1j**	92.3 ± 20.4	114.3 ± 23.6
9	**2i**	19.6 ± 3.3	5.6 ± 1.5	20	**1n**	69.4 ± 11.0	64.7 ± 21.6
10	**2j**[b]	**0.4 ± 0.1**	**2.1 ± 0.4**	21	**1p**	94.9 ± 6.5	322.4 ± 76.3
11	**2k**	224.7 ± 34.1	44.3 ± 9.5	22	**Cisplatin**	13.8 ± 1.3	5.3 ± 0.3

[a]Values were determined after 48 h of incubation. [b] The IC_{50} values of **2j** and **2p** in AML12 cells were 40.4 ± 8.5 and 38.6 ± 14.9 μM. [c] The maximum growth inhibition rate of **2n** on AML12 cells was 58%

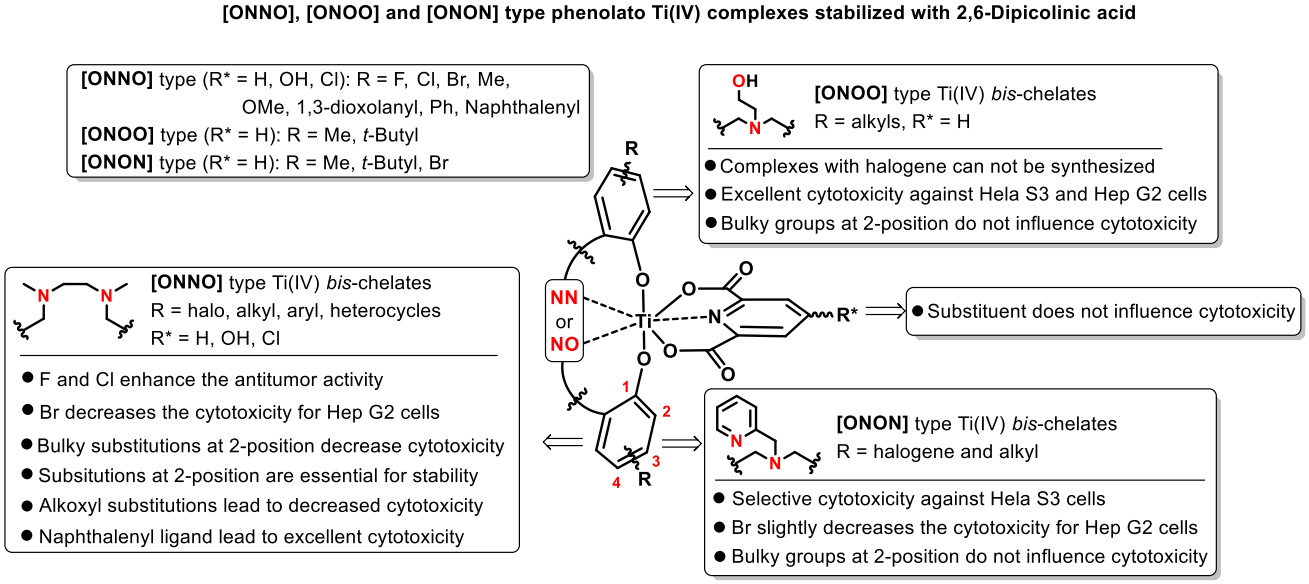

Fig. 3 Structure–activity relationship of [ONNO], [ONOO] and [ONON] amino-*bis*(phenolato) Ti(IV) *bis*-chelates

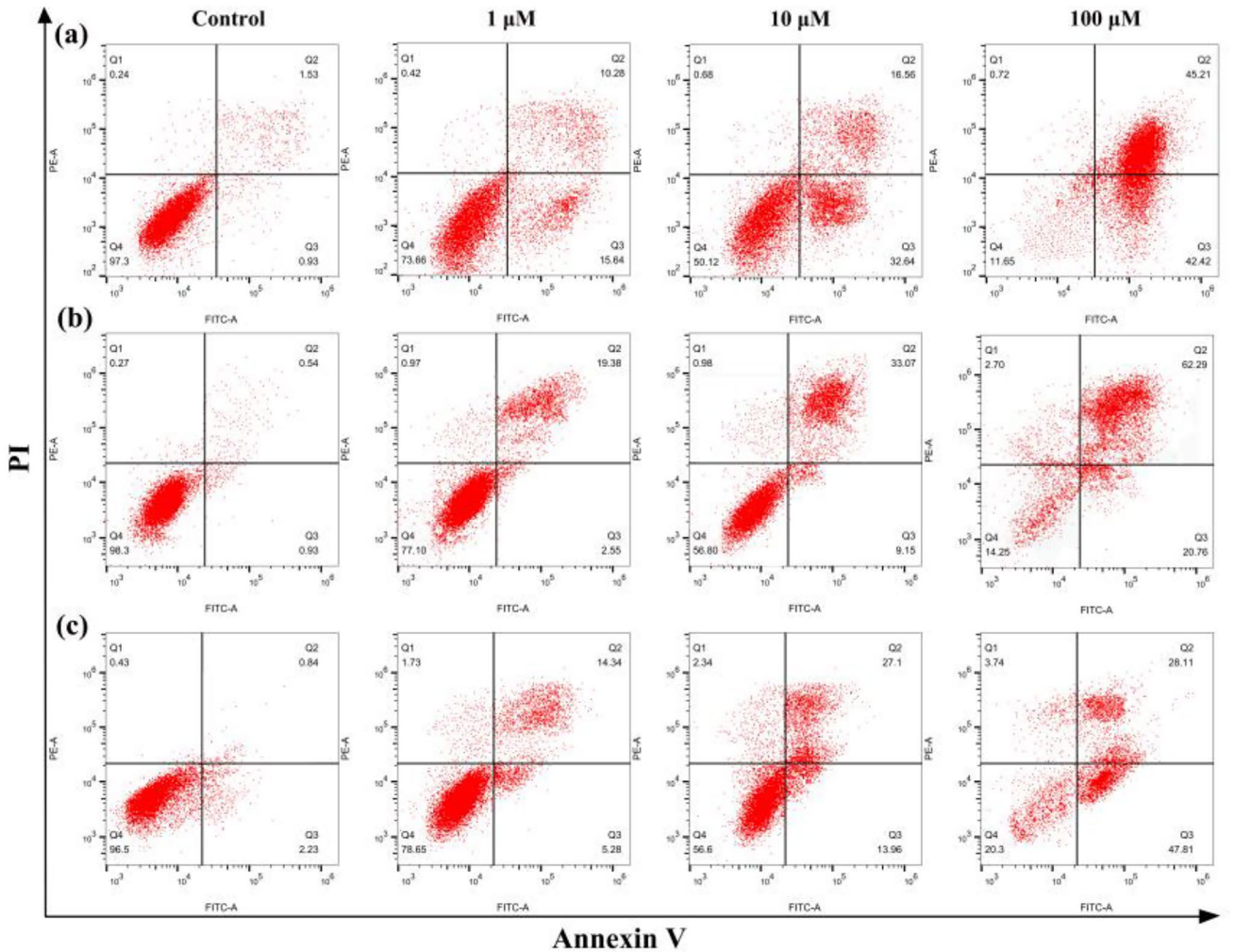

Fig. 4 Investigation of cell death by the Annexin V-FITC/PI apoptosis assay in Hela S3 cells after **2j**, **2n** and **2p** (1 μM, 10 μM and 100 μM) treatment for 48 h. **a**: **2j**, **b**: **2n**, **c**: **2p**. Quantification of necrotic (Q1), late apoptotic (Q2), early apoptotic (Q3) and viable (Q4)

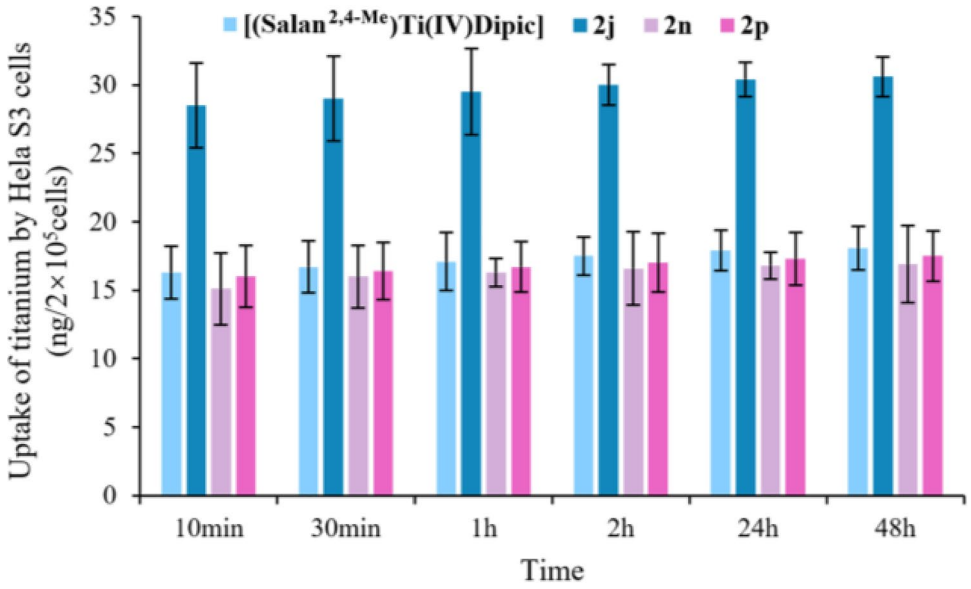

Fig. 5 Absolute cellular uptake of titanium after incubating Hela S3 cells with **[(Salan$^{2,4-Me}$)Ti(IV)Dipic]**, **2j**, **2n**, **2p** (2 μM) at given time at 37 °C. (mean ± SD) ($n = 3$)

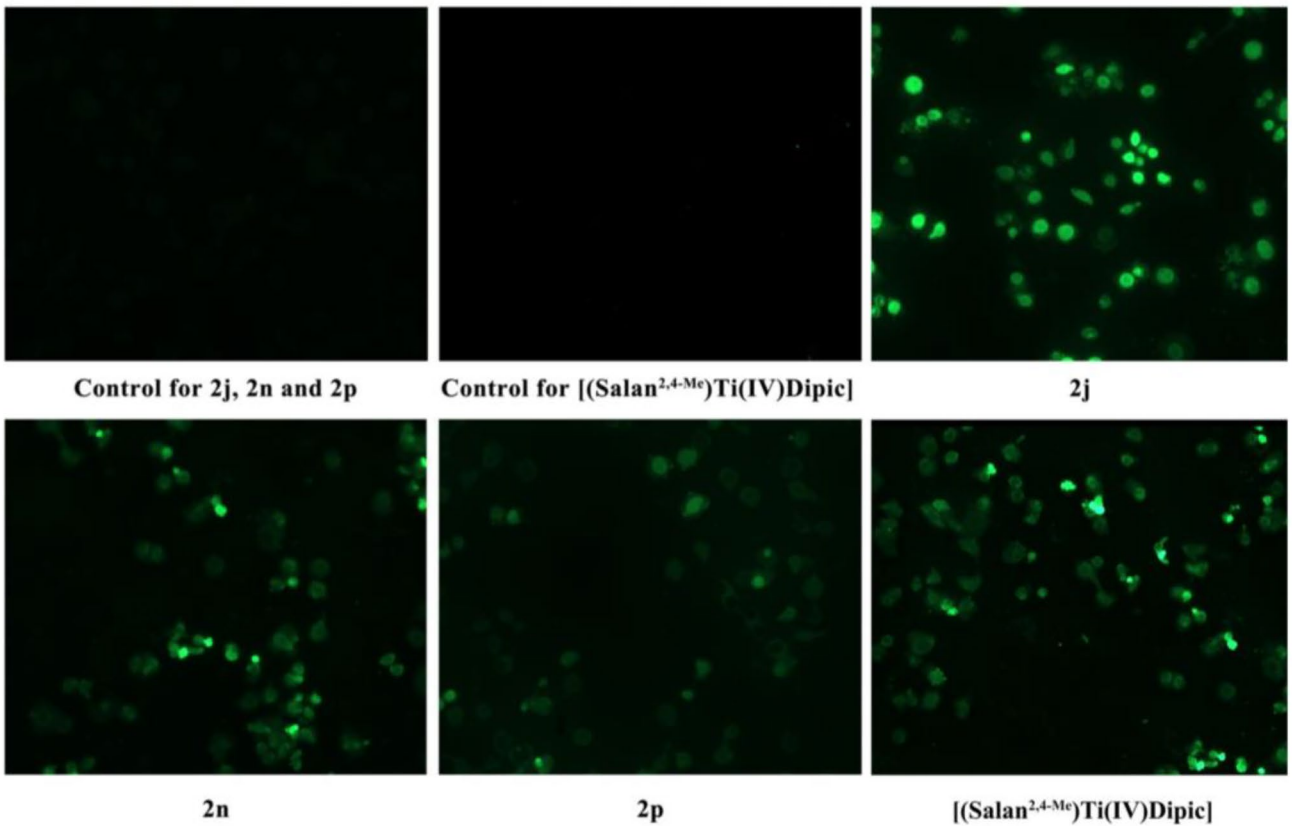

Fig. 6 Fluorescence microscopic images of intracellular ROS levels analyzed by H_2DCFDA probe after 24 h of incubation with compounds **2j**, **2n**, **2p** and **[(Salan$^{2,4-Me}$)Ti(IV)Dipic]** for Hela S3 cells. The green spots are the cell images which are stained with DCF

antitumor spectrum, mechanism of action and toxicity are to be investigated in further studies.

Supplementary Information The online version contains supplementary material available at https://doi.org/10.1007/s00775-024-02059-9.

Acknowledgements We are grateful to the demonstration project of Haizhi Plan provided by Gansu Science and Technology Association (No. GSHZSF2023-03), Science and Technology Department of Gansu Province (No. 21YF5FA082) and Department of Education of Gansu Province: Graduate Students Creation New Star (No. 2023CXZX-501) for funding of this project. Lanzhou University of Technology is greatly acknowledged for general support. The authors thank Dr. Xianggao Meng from Central China Normal University for useful discussion in the X-Ray analysis.

Funding This research was funded by the demonstration project of Haizhi Plan provided by Gansu Science and Technology Association (No. GSHZSF2023-03), Science and Technology Department of Gansu Province (No. 21YF5FA082) and Department of Education of Gansu Province: Graduate Students Creation New Star (No. 2023CXZX-501).

Data availability CCDC 2118288 (**2f**), CCDC 2132229 (**2 h**), CCDC 2183752 (**2n**), CCDC 2183480 (**2q**). Copies of the data can be obtained free of charge on application to CCDC, 12 Union Road, Cambridge CB21EZ, U.K. (fax: (+44) 1223 – 336 – 033. e-mail: deposit@ccdc.cam.ac.uk or https://www.ccdc.cam.ac.uk/structures/). Supplementary data associated with this article can be found in the online version.

Declarations

Conflict of interest The authors declare no conflict of interest.

References

1. Simpson PV, Desai NM, Casari I, Massi M, Falasca M (2019) Metal-based antitumor compounds: beyond cisplatin. Future Med Chem 11:119–135. https://doi.org/10.4155/fmc-2018-0248
2. Wilson JJ, Lippard SJ (2014) Synthetic methods for the preparation of platinum anticancer complexes. Chem Rev 114:4470–4495. https://doi.org/10.1021/cr4004314
3. de Vries G, Rosas-Plaza X, van Vugt M, Gietema JA, de Jong S (2020) Testicular cancer: Determinants of cisplatin sensitivity and novel therapeutic opportunities. Cancer Treat Rev 88:102054. https://doi.org/10.1016/j.ctrv.2020.102054
4. Shi Z-d, Hao L, Han X-x, Wu Z-x, Pang K, Dong Y, Qin J-x, Wang G-y, Zhang X-m, Xia T, Liang Q, Zhao Y, Li R, Zhang S-q, Zhang J-h, Chen J-g, Wang G-c, Chen Z-s, Han C-h (2022) Targeting HNRNPU to overcome cisplatin resistance in bladder cancer. Mol Cancer 21:37. https://doi.org/10.1186/s12943-022-01517-9
5. Wang X-h, Wang X-y, Jin S-x, Muhammad N, Guo Z-j (2019) Stimuli-responsive therapeutic metallodrugs. Chem Rev 119:1138–1192. https://doi.org/10.1021/acs.chemrev.8b00209
6. Muhammad N, Guo Z-j (2014) Metal-based anticancer chemotherapeutic agents. Curr Opin Chem Biol 19:144–153. https://doi.org/10.1016/j.cbpa.2014.02.003
7. Lu Y-l, Ma X-y, Chang X-y, Liang Z-l, Lv L, Shan M, Lu Q-y, Wen Z-f, Gust R, Liu W-k (2022) Recent development of gold(i) and gold(iii) complexes as therapeutic agents for cancer diseases. Chem Soc Rev 51:5518–5556. https://doi.org/10.1039/D1CS00933H
8. Schneider F, Zhao T-k, Huhn T (2016) Cytotoxic heteroleptic hepta-coordinate salan zirconium-(IV)-*bis*-chelates – synthesis, aqueous stability and X-ray structure analysis. ChemComm 52:10151–10154. https://doi.org/10.1039/C6CC05359A
9. Köpf H, Köpf-Maier P (1979) Titanocene dichloride–the first metallocene with cancerostatic activity. Angew Chem Int Ed 18:477–478. https://doi.org/10.1002/anie.197904771
10. Meker S, Braitbard O, Hall MD, Hochman J, Tshuva EY (2016) Specific design of titanium(IV) phenolato chelates yields stable and accessible, effective and selective anticancer agents. Chem Eur J 22:9986–9995. https://doi.org/10.1002/chem.201601389
11. Tshuva EY, Miller M (2018) 8. Coordination Complexes of Titanium(IV) for Anticancer Therapy. Metallo-Drugs: Development and Action of Anticancer Agents. Boston: De Gruyter Berlin, pp: 219–250. https://doi.org/10.1515/9783110470734-008
12. Caruso F, Rossi M (2004) Antitumor titanium compounds. Mini-Rev Med Chem 4:49–60. https://doi.org/10.2174/1389557043487565
13. Shavit M, Peri D, Manna CM, Alexander JS, Tshuva EY (2007) Active cytotoxic reagents based on non-metallocene non-diketonato well-defined C2-symmetrical titanium complexes of tetradentate bis(phenolato) ligands. J Am Chem Soc 129:12098–12099. https://doi.org/10.1021/ja0753086
14. Peri D, Manna CM, Shavit M, Tshuva EY (2011) Ti(IV) complexes of branched diamine bis(phenolato) ligands: hydrolysis and cytotoxicity. Eur J Org Chem 2011:4896–4900. https://doi.org/10.1002/ejic.201100725
15. Meker S, Margulis-Goshen K, Weiss E, Magdassi S, Tshuva EY (2012) High antitumor activity of highly resistant salan–titanium(IV) complexes in nanoparticles: an identified active species. Angew Chem Int Ed Engl 51:10515–10517. https://doi.org/10.1002/anie.201205973
16. Nahari G, Tshuva EY (2021) Synthesis of asymmetrical diaminobis(alkoxo)-bisphenol compounds and their C1-symmetrical mono-ligated titanium(iv) complexes as highly stable highly active antitumor compounds. Dalton Trans 50:6423–6426. https://doi.org/10.1039/D1DT00219H
17. Ganot N, Briaitbard O, Gammal A, Tam J, Hochman J, Tshuva EY (2018) In vivo anticancer activity of a nontoxic inert phenolato titanium complex: high efficacy on solid tumors alone and combined with platinum drugs. ChemMedChem 13:2290–2296. https://doi.org/10.1002/cmdc.201800551
18. Ganot N, Tshuva EY (2018) In vitro combinations of inert phenolato Ti(iv) complexes with clinically employed anticancer chemotherapy: synergy with oxaliplatin on colon cells. RSC Adv 8:5822–5827. https://doi.org/10.1039/C8RA00229K
19. Nahari G, Braitbard O, Larush L, Hochman J, Tshuva EY (2021) Effective oral administration of an antitumorigenic nanoformulated titanium complex. ChemMedChem 16:108–112. https://doi.org/10.1002/cmdc.202000384
20. Immel T, Grützke M, Späte AK, Groth U, Öhlschlaeger P, Huhn T (2012) Synthesis and X-ray structure analysis of a heptacoordinate titanium(IV)-bis-chelate with enhanced in vivo antitumor efficacy. ChemComm 48:5790–5792. https://doi.org/10.1039/C2CC31624B
21. Grützke M, Zhao T-k, Immel TA, Huhn T (2015) Heptacoordinate heteroleptic salan (ONNO) and thiosalan (OSSO) titanium(IV) complexes: investigation of stability and cytotoxicity. Inorg Chem 54:6697–6706. https://doi.org/10.1021/acs.inorgchem.5b00690
22. Severin GW, Nielsen CH, Jensen AI, Fonslet J, Kjær A, Zhuravlev F (2015) Bringing radiotracing to titanium-based antineoplastics: solid phase radiosynthesis, PET and ex vivo evaluation of antitumor agent [^{45}Ti](salan)Ti(dipic). J Med Chem 58:7591–7595. https://doi.org/10.1021/acs.jmedchem.5b01167

23. Zhao T-k, Wang P, Liu N, Li S-j, Yang M-j, Yang Z-d (2022) Facile synthesis of [ONON] type titanium(IV) bis-chelated complexes in alcoholic solvents and evaluation of anti-tumor activity. J Inorg Biochem 235:111925. https://doi.org/10.1016/j.jinorgbio.2022.111925
24. Zhao T-k, Wang P, Ji M-y, Li S-j, Yang M-j, Pu X-y (2021) Post-synthetic modification research of salan titanium *bis*-chelates via sonogashira reaction. Acta Chim Sinica 79:1385–1393. https://doi.org/10.6023/A21060282
25. Zhao T-k, Wang P, Zhang X-p, Liu N, Zhao W-z, Zhang Y, Yuan P-p, Li S-j, Yang M-j, Yang Z-d, Huhn T (2023) Anti-tumoral titanium(IV) complexes stabilized with phenolato ligands and structure-activity relationship. Curr Top Med Chem 23:1835–1849. https://doi.org/10.2174/1568026623666230505104626
26. Zhao T-k, Grützke M, Götz KH, Druzhenko T, Huhn T (2015) Synthesis and X-ray structure analysis of cytotoxic heptacoordinate sulfonamide salan titanium(iv)-*bis*-chelates. Dalton Trans 44:16475–16485. https://doi.org/10.1039/C5DT01618E
27. Immel TA, Debiak M, Groth U, Bürkle A, Huhn T (2009) Highly selective apoptotic cell death induced by halo-salane titanium complexes. ChemMedChem 4:738–741. https://doi.org/10.1002/cmdc.200900038
28. Lei X, Chelamalla N (2013) Dioxomolybdenum(VI) complexes with linear and tripodal tetradenate ligands: synthesis, structures and their use as olefin epoxidation catalysts. Polyhedron 49:244–251. https://doi.org/10.1016/j.poly.2012.10.022
29. Díaz-Urrutia C, Chen W, Crites C, Daccache J, Korobkov I, Baker RT (2015) Towards lignin valorisation: comparing homogeneous catalysts for the aerobic oxidation and depolymerisation of organosolv lignin. RSC Adv 5:70502–70511. https://doi.org/10.1039/C5RA15694G
30. Srivastav N, Mutneja R, Singh N, Singh R, Kaur V, Wagler J, Kroke E (2016) Diverse molecular architectures of Si and Sn [4.4.3.$0^{1,6}$] tridecane cages derived from a mannich base possessing semi-rigid unsymmetrical podands. Eur J Inorg Chem 2016:1730–1737. https://doi.org/10.1002/ejic.201600137
31. Systat Software, Inc. 2006 (http://www.systat.com)
32. Tree Star, Inc. 2008 (http://www.flowjo.com)
33. Oparka M, Walczak J, Malinska D, van Oppen LMPE, Szczepanowska J, Koopman WJH, Wieckowski MR (2016) Quantifying ROS levels using CM-H2DCFDA and HyPer. Methods 109:3–11. https://doi.org/10.1016/j.ymeth.2016.06.008
34. Immel TA, Groth U, Huhn T (2010) Cytotoxic titanium salan complexes: surprising interaction of salan and alkoxy ligands. Chem Eur J 16:2775–2789. https://doi.org/10.1002/chem.200902312
35. Li S-j, Wang P, Ji M-y, Yang M-j, Pu X-y, Zhao T-k (2021) The crystal structure of 6,6′-(((2-(dimethylamino)ethyl)azanediyl)bis(methylene))bis(benzo[d][1,3]dioxol-5-ol ato-κ4N, N′, O, O′)-(pyridine-2,6-dicarboxylato-N, O, O′)-titanium(IV)-dichloromethane(1/1), C27H25N3O10Ti. Z KRIST-NEW CRYST ST 236:1165–1167. https://doi.org/10.1515/ncrs-2021-0260
36. Zhao T-k, Wang P, Ji M-y, Li S-j, Yang M-j, Pu X-y (2021) The crystal structure of 1,1′-(((2 (dimethylamino)ethyl) azanediyl)bis(methylene)) bis(naphthalen-2-olato-κ4 N, N′, O, O′)-(pyridine-2,6-dicarboxylato-N, O, O′)-titanium(IV)-dichloromethane (2/1), C33H29N3O6Ti. Z KRIST-NEW CRYST ST 236:985–987. https://doi.org/10.1515/ncrs-2021-0182
37. Chmura AJ, Davidson MG, Jones MD, Lunn MD, Mahon MF, Johnson AF, Khunkamchoo P, Roberts SL, Wong SSF (2006) Group 4 complexes with aminebisphenolate ligands and their application for the ring opening polymerization of cyclic esters. Macromolecules 39:7250–7257. https://doi.org/10.1021/ma061028j
38. Padmanabhan S, Katao S, Nomura K (2007) Synthesis and structure of titanatranes containing tetradentate trianionic donor ligands of the type [(O-2,4–$R_2C_6H_{2-6}$-CH_2)$_2$(OCH_2CH_2)]N_3- and their use in catalysis for ethylene polymerization. Organometallics 26:1616–1626. https://doi.org/10.1021/om0611507
39. Behm K, Fazekas E, Paterson MJ, Vilela F, McIntosh RD (2020) Discrete Ti−O−Ti complexes: visible-light-activated, homogeneous alternative to TiO_2 photosensitisers. Chem Eur J 26:9486–9494. https://doi.org/10.1002/chem.202001678
40. Barroso S, Coelho AM, Gomez-Ruiz S, Calhorda MJ, Žižak Ž, Kaluđerović GN, Martins AM, (2014) Synthesis, cytotoxic and hydrolytic studies of titanium complexes anchored by a tripodal diamine bis (phenolate) ligand. Dalton Trans 43:17422–17433. https://doi.org/10.1039/C4DT00975D
41. Tshuva EY, Versano M, Goldberg I, Kol M, WeitmanGoldschmidt H (1999) Titanium complexes of chelating dianionic amine bis(phenolate) ligands: an extra donor makes a big difference. Z Inorg Chem Commun 2:371–373. https://doi.org/10.1016/S1387-7003(99)00096-9
42. These structurally similar complexes are: **Ti-1**: [(ONON$^{2\text{-}t\text{Bu},4\text{-Me}}$)Ti(IV)Dipic] (compd. **2b** in [23]); **Ti-2**: [(ONON$^{2\text{-Br},4\text{-Me}}$)Ti(IV)Dipic] (compd. **2n** in [23]); **Ti-3:** [(ONON$^{\text{Piperonyl}}$)Ti(IV)Dipic] (Compd. **[L^1Ti(IV)(Dipic)]** in [36]; **Ti-4:** [(ONON-$^{\text{Naphthyl}}$)Ti(IV)Dipic] (Compd. **[L^1Ti(IV)(Dipic)]** in [37]; **Ti-5:** [(ONON)$^{2,4\text{-}t\text{Bu}}$Ti(IV)(O^iPr)$_2$] (compd. Ti(O^iPr)$_2$ **2b** in [38]) **Ti-6:** [(ONOO)$^{2,4\text{-}t\text{Bu}}$Ti(IV)(O^iPr)] (Compd. **2a** in [39]); and **Ti-7**: [{(ONOO)$^{2,4\text{-}t\text{Bu}}$Ti(IV)(OMe)}$_2$O] (compd. **C5** in [40])
43. Peri D, Meker S, Manna CM, Tshuva EY (2011) Different ortho and para electronic effects on hydrolysis and cytotoxicity of diamino bis (phenolato) salan Ti (IV) complexes. Inorg Chem 50:1030–1038. https://doi.org/10.1021/ic101693v
44. Abdolmaleki S, Khaksar S, Aliabadi A, Panjehpour A, Motieiyan E, Marabello D, Faraji MH, Beihaghi M (2023) Cytotoxicity and mechanism of action of metal complexes: an overview. Toxicology 492:153516. https://doi.org/10.1016/j.tox.2023.153516
45. Zhao T-k, Wang P, Liu N, Zhao W-z, Yang M-j, Li S-j, Yang Z-d, Sun B-l, Huhn T (2023) Synthesis and X-ray structure analysis of cytotoxic heptacoordinated Salan hafnium(IV) complexes stabilized with 2,6-dipicolinic acid. J Inorg Biochem 240:112094. https://doi.org/10.1016/j.jinorgbio.2022.112094
46. Azmanova M, Pitto-Barry A (2022) Oxidative stress in cancer therapy: friend or enemy? ChemBioChem 23:e202100641. https://doi.org/10.1002/cbic.202100641
47. Shpilt Z, Melamed-Book N, Tshuva EY (2023) An anticancer Ti(IV) complex increases mitochondrial reactive oxygen species levels in relation with hypoxia and endoplasmic-reticulum stress: a distinct non DNA-related mechanism. J Inorg Biochem 243:112197. https://doi.org/10.1016/j.jinorgbio.2023.112197

Authors and Affiliations

Shanjia Li[1] · Xupeng Zhang[1] · Tiankun Zhao[1] · Nan Liu[1] · Yong Zhang[1] · Peng Wang[2] · Zhongduo Yang[1] · Thomas Huhn[3]

✉ Tiankun Zhao
zhaotiankun2006@163.com

✉ Thomas Huhn
thomas.huhn@uni-konstanz.de

[1] College of Life Science and Engineering, Lanzhou University of Technology, Lanzhou 730050, People's Republic of China

[2] School of Chemistry, Sun Yat-Sen University, Guangzhou 510006, People's Republic of China

[3] Fachbereich Chemie, Universität Konstanz, Universitätsstr. 10, 78457 Konstanz, Germany